Surface potential measurement of organic thin film on metal electrodes by dynamic force microscopy using a piezoelectric cantilever

AUTHOR(S):

Satoh, Nobuo; Katori, Shigetaka; Kobayashi, Kei; Watanabe, Shunji; Fujii, Toru; Matsushige, Kazumi; Yamada, Hirofumi

CITATION:

Satoh, Nobuo ...[et al]. Surface potential measurement of organic thin film on metal electrodes by dynamic force microscopy using a piezoelectric cantilever. Journal of Applied Physics 2011, 109(11): 114306.

ISSUE DATE:

2011

URL:

http://hdl.handle.net/2433/143576

JOURNAL OF APPLIED PHYSICS **109**, 114306 (2011)

Surface potential measurement of organic thin film on metal electrodes by dynamic force microscopy using a piezoelectric cantilever

Nobuo Satoh,[1,a)] Shigetaka Katori,[1] Kei Kobayashi,[2] Shunji Watanabe,[3] Toru Fujii,[3] Kazumi Matsushige,[1] and Hirofumi Yamada[1]
[1]*Department of Electronic Science and Engineering, Kyoto University, Katsura, Nishikyo, Kyoto 615-8510, Japan*
[2]*Office of Society-Academia Collaboration for Innovation, Kyoto University, Katsura, Nishikyo, Kyoto 615-8520, Japan*
[3]*Nikon Corporation, 1-10-1 Asamizodai, Sagamihara, Kanagawa 228-0828, Japan*

(Received 8 February 2011; accepted 1 April 2011; published online 6 June 2011)

We describe applications of a cantilever with a lead zirconate titanate (PZT) piezoelectric film as self-sensing to dynamic force microscopy (DFM) combined with Kelvin probe force microscopy (KFM). We adopted a frequency modulation (FM) detection method not only to stabilize the imaging conditions in our DFM but also to enhance the sensitivity for the detection of electrostatic forces in KFM measurement. We deposited Alq_3 [tris (8-hydroxyquinolinato) aluminum] thin films and aluminum (Al) electrode patterns on an indium tin oxide (ITO)/glass substrate by vacuum evaporation using shadow masks. The surface structures and local surface potential of Alq_3 films on metals were investigated using our DFM/KFM instrument to study the local electrical properties at the molecule–metal interface. The photosensitive organic material sample can be in a completely dark environment because no optics are required for cantilever deflection sensing in our experimental setup. © *2011 American Institute of Physics*. [doi:10.1063/1.3585865]

I. INTRODUCTION

Active devices such as organic light-emitting diodes (OLEDs),[1–5] organic field-effect transistors (OFETs),[6,7] and organic solar cells[8–10] have various features, including light weight, low-cost process, and flexibility. These devices consist of organic semiconductor materials. There have been a large number of studies on semiconducting molecules that have demonstrated a wide variety of electrical and optical properties. Organic thin films with different characteristics have been accumulated with a thickness of several nanometers. These devices have a bonded interface of "organic/organic" and "organic/inorganic" (e.g., metal electrode). The characteristics (luminescence efficiency, charge motility, photoelectric conversion, etc.) of these organic semiconductor devices greatly depend on the interface structures.[11–14] Therefore, in order to realize efficient devices, it is important to understand the charge potential on the surfaces and the interfaces in laminated thin films.

Scanning probe microscopy (SPM) has been a powerful tool not only for imaging surface topography but also for investigating material properties on a nanometer-scale resolution. Atomic force microscopy (AFM) is the only method that enables nano- to atomic-scale resolution on insulating surfaces in real space.[15] This feature is particularly important in terms of its applications to organic thin films, which often have poor electrical conductivity. Kelvin probe force microscopy (KFM)[16] is one of the applications of SPM. The local surface potential of films can be mapped in vacuum by KFM, and then applied to a variety of semiconducting material samples, such as organic molecules, from metal to insulator ones. The combined dynamic force microscopy (DFM) and KFM microscope can measure the surface structure and surface potential simultaneously on the same area.

We have developed multifunction SPM using a microfabricated cantilever with a lead zirconate titanate (PZT) piezoelectric thin film used as a deflection sensor applied to dynamic-mode AFM.[17–19] The cantilever is referred to as a PZT cantilever. The scattered light of the laser beam used for the displacement sensing in conventional AFM may be a noise source. In particular, it causes difficulty in the observation of photosensitive materials. The observation sample can be in a completely dark environment because no optics are required for cantilever deflection sensing in our experimental setup.

We adopted a frequency modulation (FM) detection method[20] not only to stabilize the imaging conditions in dynamic-mode operation, but also to enhance the sensitivity for the detection of electrostatic forces in KFM measurement. Furthermore, the interaction forces measured by dynamic-mode AFM using FM detection are classified into two categories: conservative and dissipative.[21,22] The conservative forces induce a frequency shift of the cantilever resonance, whereas the dissipative forces cause an amplitude variation of the cantilever oscillation. The energy dissipation process of the cantilever vibration energy has attracted much attention due to the importance of understanding the dynamic behavior at the tip as it approaches the sample surface.

In this study, we prepared an indium tin oxide (ITO)/glass substrate, and deposited aluminum (Al) metal electrode patterns and Alq_3 [tris (8-hydroxyquinolinato) aluminum] thin film patterns by vacuum evaporation with two shadow masks in each crossed direction. The measurements in a vacuum condition were carried out using the FM detection technique, which employed DFM. We investigated the organic thin film

[a)]Electronic mail: n-satoh@kuee.kyoto-u.ac.jp.

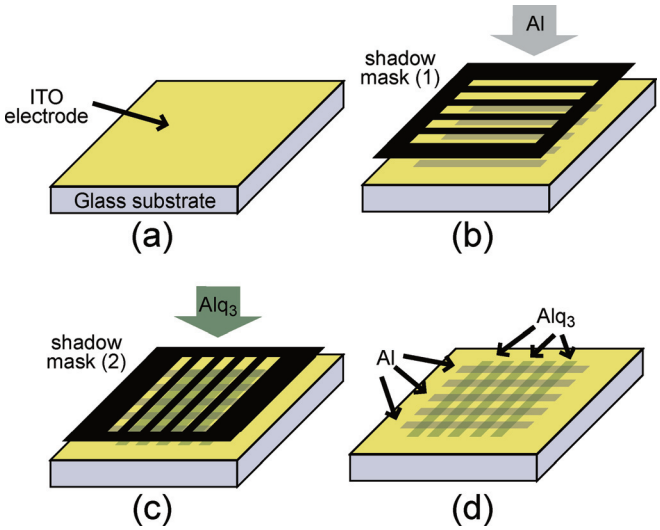

FIG. 1. (Color online) Sample making method. (a) Washing and cleaning (b) Deposition of aluminum using shadow mask (c) Deposition of Alq_3 using another shadow mask (d) Sample with intersecting area.

deposited on the metal surface to explore the possible applications of our SPM instrument using a piezoelectric cantilever.

II. EXPERIMENTAL

A. Sample preparation

Figure 1 depicts the fabrication process of the DFM/KFM observation sample. We purchased ITO-coated glasses (Kuramoto Seisakusho Co., Ltd.) as the sample substrate. We removed the contamination on the surface substrate by ultrasonic cleansing that used acetone and isopropyl alcoholic solutions as well as UV-ozone cleaning. Immediately after treatment, the substrate was placed in the vacuum evaporation system (Eiko Engineering Co., Ltd.; EO-5) to deposit the Al and Alq_3 thin films. The deposition rate was monitored using a quartz crystal micro balance.

Al electrode film was deposited from a crucible of aluminum source using a shadow mask (1) under the vacuum pressure condition of 1.5×10^{-3} Pa [Fig. 1(b)]. The temperature of the crucible was maintained at 1100°C during the deposition. The deposition rate of Al was adjusted to 0.2 nm/s. The shadow mask (1), which was made of stainless steel, had line and space patterns with a pitch of 30 μm (Toyo Precision Part Mfg. Co., Ltd.). Subsequently, Alq_3 molecules were deposited from a crucible of Alq_3 source using a shadow mask (2) under the vacuum pressure condition of 3.9×10^{-4} Pa [Fig. 1(c)]. The temperature of the crucible was maintained at 310°C during the deposition. The deposition rate of Alq_3 was adjusted to 0.1 nm/s. The shadow mask (2) used for the deposition of Alq_3 molecules had line and space patterns in the direction differed by 90° to those of the mask used for Al deposition. Each film was deposited as a result of the intersecting shape layers. Finally, it was deposited on the ITO/glass substrate as a film in which the line pattern of Alq_3 intersected with that of the aluminum film [Fig. 1(d)].

The sample was retrieved from the vacuum evaporation chamber and then placed in the DFM/KFM system. The sample was exposed to atmosphere but was protected from any light by wrapping in aluminum foil during the transfer. Figure 2 presents an optical microscope image of the sample surface obtained by the charge coupled device (CCD) camera of the DFM/KFM system. This image depicts the intersection of two shadow masks (Al electrode films and Alq_3 thin films, as shown in Fig. 1). The appearance that intersects in the deposition of the molecules in the line pattern of each thin film, which is accumulated, can be confirmed. The approximately 30 μm pitch of width in the line and space on the sample is confirmed in the optical microscope image. The position of the AFM cantilever was adjusted to the part of the intersection point of the four areas; Alq_3/Al/ITO, Alq_3/ITO, Al/ITO, and ITO.

B. Instrumentation

Figure 3 depicts an experimental setup for DFM/KFM measurements using the PZT cantilever. A commercially available AFM (SII Nanotechnology Inc.; SPA300HV) was used as an equipment base. The PZT cantilever was mounted on a laboratory-built cantilever holder. Dynamic mode AFM was operated in a vacuum environment under a pressure of approximately 1×10^{-4} Pa at room temperature. All measurements were performed in a dark environment in order to avoid photovoltaic effects.[23]

The PZT cantilever beam was made of silicon. The tip, which was located at the end of the beam, was a silicon nitride hollow pyramid. A 200-nm-thick platinum film as the lower electrode, an 800-nm-thick PZT film as a deflection sensing layer, and another platinum layer as the upper electrode were formed. In order to perform KFM measurement, a 20-nm-thick platinum film was sputter-deposited on the tip side to make the tip conductive. The radius of the apex and the tip angle were less than 50 nm and 40°, respectively. Typical resonance frequency of the PZT cantilever ranged from 80 to 100 kHz and the spring constant was calculated to be approximately 150 N/m from its dimensions. The measured mechanical quality factor (Q-value) ranged from 1,000 to 2,000 in vacuum.

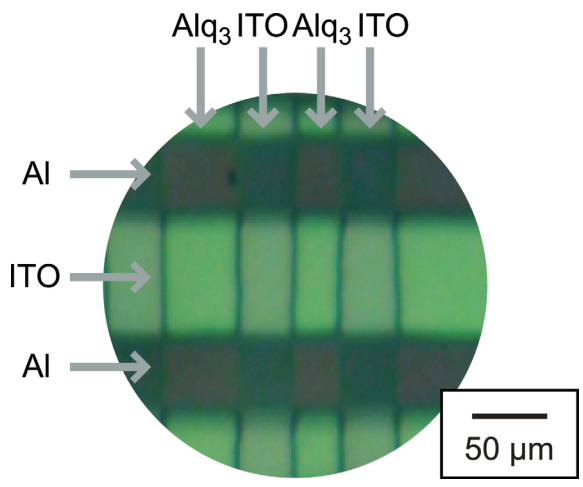

FIG. 2. (Color online) CCD image by optical microscope in DFM of the Alq_3 and the Al thin films with patterns on the ITO substrate.

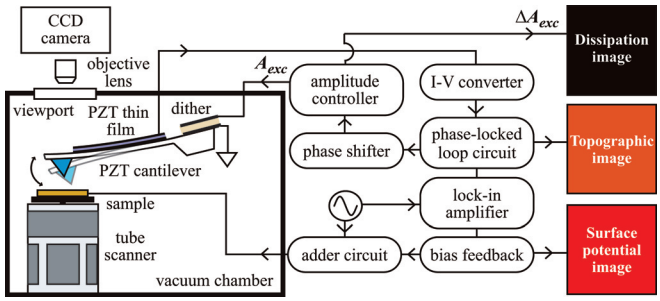

FIG. 3. (Color online) Experimental setup for DFM combined with KFM using the PZT cantilever in the vacuum chamber.

Due to the high Q-value of the cantilever in vacuum condition, the response time of the feedback circuit for the slope detection method was extremely long. Thus, slope detection is inconvenient for DFM/KFM observation in vacuum condition. However, the FM detection method, where the cantilever is used as a resonator in a self-oscillation loop, has a shorter response time independence if the Q-value of the cantilever is high. In this experiment, the tip–sample distance was regulated by the FM detection method. The cantilever was always oscillated at its resonance frequency using a self-oscillation circuit, including the cantilever as a mechanical resonator. The deflection of the PZT cantilever was detected by a current-to-voltage (I–V) converter and the resonance frequency shift was detected using a laboratory-built FM detector.[24] The gap distance of tip-sample was regulated by keeping the negative frequency shift constant, which indicates that the total interaction force is attractive.

The PZT cantilever was vibrated in the constant amplitude mode, where the vibration amplitude of the cantilever was kept constant by adjusting the amplitude of the cantilever excitation signal (A_{exc}). In this mode, energy dissipation caused by the tip-sample interaction can be estimated from the additional increase or decrease of ΔA_{exc}. Thus, an energy dissipation image was obtained as a two-dimensional map of ΔA_{exc}.

In the KFM measurement, the signal generated as displacement of the resonance frequency of the cantilever when the modulation bias voltage (2 kHz, 2 V_{p-p}) was applied between the cantilever and the sample surface is detected using a lock-in amplifier (NF Corp.; LI5640). This obtained signal is based on the electrostatic force that affected the cantilever, and this corresponds to the potential on the sample surface. Finally, the amount of the surface potential is measured by the null method compensated for by the surface charge with the potential feedback circuit. The advantage of this experimental setup is that we can simultaneously obtain a topographic image, surface potential image, and energy dissipation image in the same area. The acquisition time for obtaining images were approximately 30 mins.

III. RESULTS AND DISCUSSION

A. DFM/KFM observation results

Figures 4(a), 4(b), and 4(c) show a topographic image, a surface potential image, and an energy dissipation image, respectively, on the same area. Figure 4(a) shows a topographic image of an Alq_3 thin film and an Al electrode pattern on the ITO/glass substrate. We confirmed that the electrode thickness of Al was 95 nm and the film thickness of Alq_3 was 120 nm.

Figure 4(b) shows that surface potentials were mapped on the Alq_3, the Al electrode, their crossed regions, and the ITO electrode in a completely dark environment. Modest differences in surface potential between the organic thin film region (Alq_3) and the electrode (Al, ITO) were observed. The gradation from high potential area to low potential area corresponds to the vacuum level shift and contact potential difference between the Pt-coated probe tip and each surface of the sample. The ITO electrode region where the work function is 4.8 eV (Refs. 11 and 25) appeared in the surface potential image as a difference of +0.5 V because the work function difference with the Pt-coated cantilever whose work function is approximately 5.3 eV[26] was 0.5 eV. According to a similar consideration, the surface potential on the Al electrode region where the work function is approximately 4.3 eV (Ref. 27) was obtained as +1.0 V because the work function difference with the Pt-coated cantilever and Al area was 1.0 eV. Thus, the surface potential related to 4.3 eV and

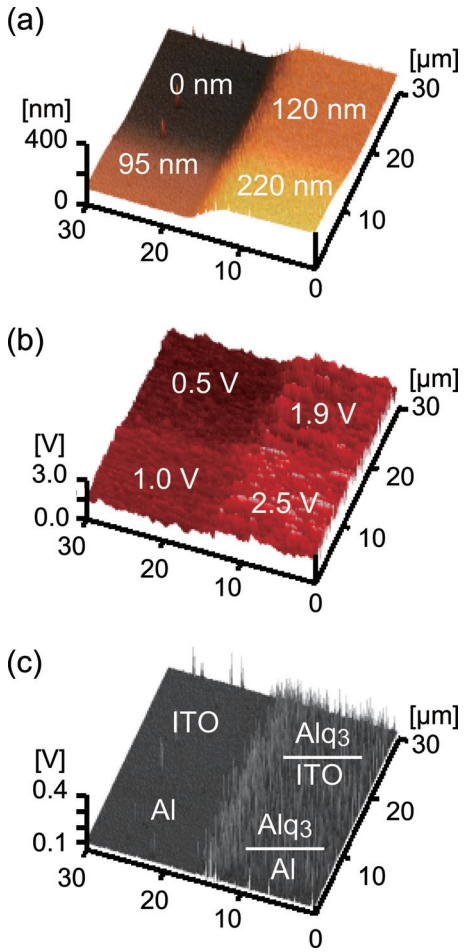

FIG. 4. (Color online) (a) Topographic image of Alq_3 thin film and Al electrode pattern on the ITO/glass substrate (30 μm × 30 μm, $\Delta f = -10$ Hz). (b) Surface potential image of the same area obtained by KFM. (c) Dissipation image of the same area measured by the gain controller in DFM.

4.8 eV, which was each work function, was detected as the area of Al and ITO electrodes, respectively. The Alq_3 film, which is the organic semiconductor, was observed with +2.5 V on the Al electrode and +1.9 V on the ITO electrode. It can be confirmed that a vacuum level shift of approximately +1.5 V was generated regardless of the kind of electrode material as a result.

Figure 4(c) presents an energy dissipation image of the same area. Dissipative forces reduce the cantilever vibration amplitude, which means that the kinetic energy of the cantilever is dissipated through tip-sample interactions. The energy dissipation measured on the Al and ITO electrodes is smaller than that on the Alq_3 organic semiconductor layer area. Thus, the energy dissipation changes when the probe tip scans different areas. Here, it was assumed that there is no atomic-scale change in the structure of the tip,[28] so that dissipation of the cantilever kinetic energy is due only to different surface properties. For organic thin films, structural fluctuations are more relevant because molecules are loosely packed[29] or have disordered structure and so, thin films are not as firm as the inorganic surfaces. In this experiment, when the probe tip scans with a relatively small resonance frequency shift,[30] the energy dissipation is relatively small and the amplitude regulation circuit can respond quickly enough to suppress the transient response of the tip sample distance regulation feedback loop, which is typically responsible for inducing topographic artifacts.

B. Energy band diagram

In the interface of the electrode and the organic semiconductor, it is assumed that the vacuum level shift occurred because the interfacial electric double layer was formed by the molecule having a dipole.[11,31] The energy band diagram is depicted from the obtained topographic image and surface potential image. Because the behavior of the band bending at the interfaces is not well known, the energy band diagram was represented with a flatband condition. It was sufficiently thick compared with the film thickness that would result in band bending.

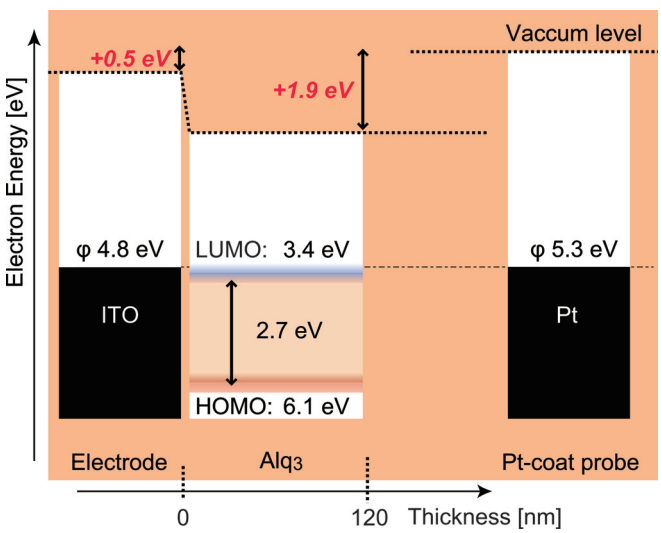

FIG. 5. (Color online) Energy band diagram in the state that the film was formed on ITO electrode.

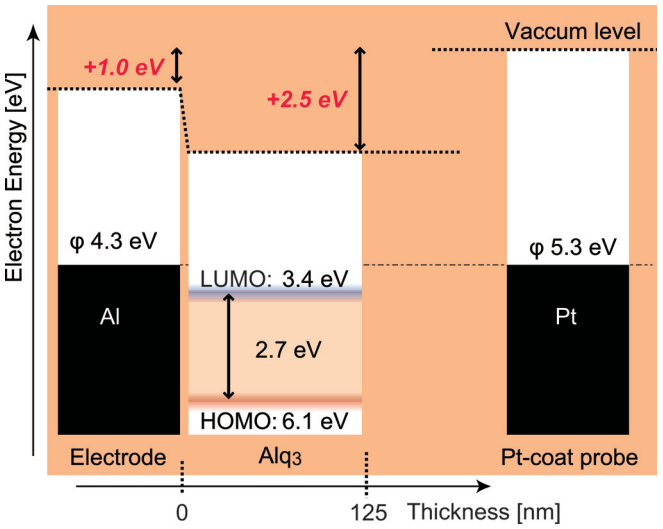

FIG. 6. (Color online) Energy band diagram in the state that the film was formed on aluminum electrode.

The Alq_3 film on ITO as the anode and the Pt-coated probe in the energy band diagram are shown from the obtained topographic image and surface potential image in Fig. 5. The Pt probe corresponds to the Fermi level potential for the ITO electrode. The Alq_3 HOMO level was shown from the amount of the vacuum level shift of the Pt probe and the Alq_3 film at the same level as the Fermi level potential in Fig. 5. The Alq_3 molecular film is LUMO: 3.4 eV and HOMO: 6.1 eV (Ref. 32).

The Alq_3 film on aluminum as the cathode and the Pt-coated probe in the energy band diagram are shown from the obtained topographic image and the surface potential image in Fig. 6. The Pt probe corresponds to the Fermi level potential for the Al electrode, and it is shown that the Alq_3 HOMO level is located below the Fermi level potential from the amount of the vacuum level shift of the Pt probe and the Alq_3 film. It is shown that the career migration of the electron can happen from the Al cathode to the Alq_3 film more easily than in the ITO electrode in the band diagrams.

IV. CONCLUSIONS

A microfabricated cantilever with PZT thin film used as an integrated deflection sensor was applied to dynamic-mode AFM/KFM. DFM/KFM observation can be conducted in a completely dark environment because no optical components are required for the cantilever deflection measurement. We succeeded in simultaneously determining the topography, surface potential, and energy dissipation in organic thin films on the electrode. Surface potentials were mapped on an Alq_3, an Al electrode, their crossed regions, and an ITO substrate. The organic thin films were provided extra energy through the dissipative tip-sample interaction.

ACKNOWLEDGMENTS

The authors would like to thank Dr. Masayuki Yahiro of Kyushu University for his helpful discussion, especially in

consideration of organic/inorganic interfacial phenomenon, and to acknowledge the Kyoto University Venture Business Laboratory Project. This research was partially supported by the Global Center of Excellent program of Kyoto University (C09), National Institute of Information and Communications Technology, and a Grant-in-Aid for Young Scientists (B) (Grant No. 20760469) from the Ministry of Education, Culture, Sports, Science and Technology of Japan.

[1]P. S. Vinceett, W. A. Barlow, R. A. Hann, and G. G. Roberts, Thin Solid Films **94**, 171 (1982).
[2]S. Hayashi, H. Etoh, and S. Saito, Jpn. J. Appl. Phys. **25**, L773 (1986).
[3]C. W. Tang, and S. A. VanSlyke, Appl. Phys. Lett. **51**, 913 (1987).
[4]J. Kido, M. Kimura, and K. Nagai, Science **267**, 1332 (1995).
[5]H. Fukagawa, K. Watanabe, T. Tsuzuki, and S. Tokito, Appl. Phys. Lett. **93**, 133312 (2008).
[6]A. Tsumura, H. Koezuka, and T. Ando, Appl. Phys. Lett. **49**, 1210 (1986).
[7]T. Manaka, F. Liu, M. Weis, and M. Iwamoto, Phys. Rev. B **78**, 121302 (2008).
[8]C. W. Tang, Appl. Phys. Lett. **48**, 183 (1986).
[9]L. S. Mende, A. Fechtenkotter, K. Mullen, E. Moons, R. H. Friend, and J. D. MacKenzie, Science **293**, 1119 (2001).
[10]H. Hoppe, and N. S. Sariciftci, J. Mater. Res. **19**, 1924 (2004).
[11]H. Ishii, K. Sugiyama, E. Ito, and K. Seki, Adv. Mater. **11**, 605 (1999).
[12]C. Adachi, M. A. Baldo, M. E. Thompson, and S. R. Forrest, J. Appl. Phys. **90**, 5048 (2001).
[13]S. Tokito, T. Iijima, Y. Suzuri, H. Kita, T. Tsuzuki, and F. Sato, Appl. Phys. Lett. **83**, 569 (2003).
[14]J. C. Scott, J. Vac. Sci. Technol. A **21**, 521 (2003).
[15]C. F. Quate, Jpn. J. Appl. Phys. **42**, 4777 (2003).
[16]M. Nonnenmacher, M. P. O'Boyle, and H. K. Wickramasinghe, Appl. Phys. Lett. **58**, 2921 (1991).
[17]T. Fujii and S. Watanabe, Appl. Phys. Lett. **68**, 467 (1996).
[18]K. Kobayashi, H. Yamada, K. Umeda, T. Horiuchi, S. Watanabe, T. Fujii, S. Hotta, and K. Matsushige, Appl. Phys. A **72**, 97 (2001).
[19]N. Satoh, K. Kobayashi, S. Watanabe, T. Fujii, T. Horiuchi, H. Yamada, and K. Matsushige, Jpn. J. Appl. Phys. **42**, 4878 (2003).
[20]T. R. Albrecht, P. Gräutter, D. Horne, and D. Rugar, J. Appl. Phys. **69**, 668 (1991).
[21]B. Gotsmann, C. Seidel, B. Anczykowski, and H. Fuchs, Phys. Rev. B **60**, 11051 (1999).
[22]M. Guggisberg, M. Bammerlin, Ch. Loppacher, O. Pfeiffer, A. Abdurixit, V. Barwich, R. Bennewitz, A. Baratoff, E. Meyer, and H.-J. Guntherodt, Phys. Rev. B **61**, 11151 (2000).
[23]E. Ito, Y. Washizu, N. Hayashi, H. Ishii, N. Matsuie, K. Tsuboi, Y. Ouchi, Y. Harima, K. Yamashita, and K. Seki, J. Appl. Phys. **92**, 7306 (2002).
[24]K. Kobayashi, H. Yamada, H. Itoh, T. Horiuchi, and K. Matsushige, Rev. Sci. Instrum. **72**, 4383 (2001).
[25]K. Sugiyama, H. Ishii, Y. Ouchi, and K. Seki, J. Appl. Phys. **87**, 295 (2000).
[26]R. Bouwman, and W. M. H. Sachtler, J. Catal. **19**, 127 (1970).
[27]R. M. Eastmenti, and C. H. B. Mee, J. Phys. F: Met. Phys. **3**, 1738 (1973).
[28]R. Bennewitz, A. S. Foster, L. N. Kantrovich, M. Bammerlin, C. Loppacher, S. Schär, M. Guggisberg, and E. Meyer, Phys. Rev. B **62**, 013674 (2000).
[29]T. Fukuma, K. Kobayashi, H. Yamada, and K. Matsushige, J. Appl. Phys. **95**, 4742 (2004).
[30]T. Ichii, T. Fukuma, K. Kobayashi, H. Yamada, and K. Matsushige, Appl. Surf. Sci. **210**, 99 (2003).
[31]I. G. Hill, A. Rajagopal, A. Kahn, and Y. Hu, Appl. Phys. Lett. **73**, 662 (1998).
[32]I. G. Hill, and Y. Hu, J. Appl. Phys. **84**, 5583 (1998).